Download Alleviation of a Tilt-rotor Wing by Active Flow Control Strategies

P. KJELLGREN[1,2], M. EL-ALTI[2], and L. DAVIDSON[2]
[1]Per Kjellgren Engineering, Nyvollhagen 9, 4070 Randaberg, Norway
[2]Division of Fluid Dynamics, Dept. of Applied Mechanics, Chalmers University of Technology, Gothenburg, Sweden

Summary

A part of the current flow control research at Chalmers University is directed towards aerodynamic drag reduction of bluff bodies using zero mass-flux oscillatory jets. The goal is to develop and test a functional prototype to be used on a truck, and to improve current numerical methods for analyzing such cases. As a first step, we investigated the widely published case of active flow control on the tilt-rotor XV-15 wing. Large eddy simulations were carried out for cases with and without active flow control, and with the help of numerical design and shape optimization tools, drag reductions of 30%-45% were achieved.

1 Introduction

Tilt-rotor aircrafts have significant performance advantages to standard helicopters, with more than twice the speed and maximum flight altitude and more than 3 times longer range of flight. However, in hover conditions the airstreams from the rotors impinge on the tilt-rotor aircraft wing surfaces and parts of the fuselage, resulting in a loss of lifting capability. Research programs using passive flow control techniques have been carried out at NASA, Bell, and Boeing in an attempt to reduce the download drag [1, 2, 3, 4]. These studies showed that the only practical passive control was to use a trailing edge flap, which was deflected during hover. This was also used for the experimental proof-of-concept XV-15 aircraft. However, even with a trailing edge flap, the loss, or the download drag, was still approximately 10% of the weight of the aircraft, almost equal to the design payload for a fully tanked tilt-rotor aircraft.

A deflected trailing edge flap reduces the exposed area and the flow remains attached at modest flap angles, leading to a smaller wake. With the help of active flow control (AFC), the flap can be deflected even further without risking flow separation, making the wake and thereby the drag even smaller.

Zero mass-flux oscillatory jet actuators were implemented into an XV-15 and full-scale test-flights were carried out during the summer-2003. The tests were a success, and were noticed even by mainstream aviation media [5,6].

From a numerical point of view, even without any AFC, calculating time-dependent turbulent flow past a bluff body with non-trivial geometry is a challenge. The addition of AFC makes it even more so. The forcing slot is typically very narrow, the slot peak velocities are considerably higher than the freestream velocity, and it oscillates at frequencies much higher than the Strouhal frequency. The high spatial and temporal accuracy and also generality of LES makes it a good candidate for this kind of flow, and was successfully used in the tilt-rotor airfoil calculations [7,8,9] and more recently also in [10].

2 Numerical Method

Both unforced and forced cases were calculated with a semi-implicit, fractional step, finite element method with large eddy simulation turbulence models. The details of the numerical algorithm are presented in [11] and [12].

As for the LES turbulence models, both the constant as well as the dynamic coefficient Smagorinsky subgrid scale models were used. For the constant coefficient model, the Van Driest damping function was used with the wall assumed to be smooth, and for the dynamic model the Lilly approach was used [13].

2.1 Forcing Slot For Flow Control

The slot forcing is governed by slot width, angle, velocity time variation, velocity profile, and frequency. As illustrated in Figure 1a, the effective slot width h was taken as $h = T\sin\alpha$, where α is the angle of the velocity to the surface and T is the length of the slot on the surface. The oscillatory momentum coming from the slot is:

$$\langle J \rangle = \int_0^h r \langle u \rangle^2 dh . \tag{1}$$

Notice that this integral will vary depending on the numerical discretization of the underlying scheme. As for the current finite element formulation, the momentum for each element would be integrated as:

$$\langle J^e \rangle = \int_0^{\Delta h} r \left\langle \sum_k N^k u^k \right\rangle^2 dh . \tag{2}$$

For simplicity, we look at the slot boundary for a two-dimensional problem. Now, using one-point integration leads to

$$\langle J^e \rangle = \int_0^{\Delta h} r \left\langle \sum_k N^k u^k \right\rangle^2 dh = r \frac{1}{4} \left(\langle u_1 \rangle^2 + 2 \langle u_1 \rangle \langle u_2 \rangle + \langle u_2 \rangle^2 \right) \Delta h . \tag{3}$$

Assuming the slot velocity has a top-hat profile, < > denotes RMS values, Δh is constant for all slot elements, and the velocities of the first and last slot nodes are zero gives the assembled momentum as

$$\langle J \rangle = r \left(\frac{1}{4} \langle u \rangle^2 + (n-2) \langle u \rangle^2 + \frac{1}{4} \langle u \rangle^2 \right) \Delta h = r \frac{2n-3}{2} \langle u \rangle^2 \Delta h, \tag{4}$$

where n is the number of elements for the slot. Following the definition used here, the RMS momentum coefficient is

$$\langle C_m \rangle = \frac{\langle J \rangle}{chord \times \frac{1}{2} r \ u_\infty^2}, \tag{5}$$

from which the required nodal velocities at the slot are given by

$$\langle u \rangle = \sqrt{\frac{C_m \times chord \times u_\infty^2}{(2n-3)\Delta h}} = \sqrt{\frac{C_m \times chord \times u_\infty^2}{(2n-3)\Delta x \sin a}}, \tag{6}$$

where chord is the full chord of the airfoil+flap at zero degrees flap angle. Assuming that the forcing is a pure sinusoidal, we have

$$u(t) = \sqrt{2} \langle u \rangle \sin(2p Ft), \tag{7}$$

which is enforced as a Dirichlet boundary condition and where F is the forcing frequency. The non-dimensional forcing frequency F^+ is usually used, where

$$F^+ = \frac{F \times X_{TE}}{U_\infty}, \tag{8}$$

and where X_{TE} is the distance from the slot to the trailing edge of the flap.

2.2 Computational Domain & Mesh

A schematic view of the computational domain is shown in Figure 1b. For a bluff body problem, it is important to capture the vortex structure in the wake region and therefore the nodes are heavily concentrated in the boundary layer and in the near-wake region, as shown in Figure 1c. Grid spacing for the worst-case scenario, i.e. when the AFC is on which makes the boundary layer on the flap thinner, is presented in Table [1]. The number of nodes is approximately

$7e^5$-$1.4e^6$ and typically > 100,000 time steps are used. The time step varies throughout the calculation, changing every tenth time step by an automatic time stepper that keeps the Courant number constant at CFL=2.0. This corresponded to timestep sizes being in the range $2x10^{-5}$-$7x10^{-5}$ seconds.

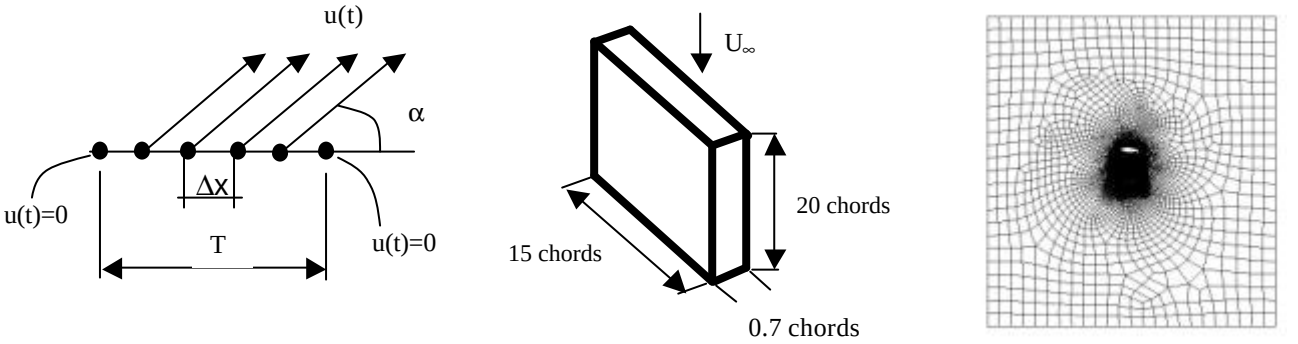

Figure 1 a) Schematic view of slot. Black dots are nodes on the boundary. b) Size and shape of computational domain c) Finite element mesh

Table 1 Mesh resolution on flap for most critical case (forcing on)

Location (% from L.E)	Δx^+	Δy^+	Δz^+
0 %	15	2.0	108
15 %	4.0	1.0	29
60 %	6.0	1.8	33

3 Results

The airfoil in download configuration is a bluff body with the characteristic global vortex shedding. An instantaneous plot of the pressure contours in a slice in the middle of the computational domain at a time when the C_d is close to a local maximum is shown in Figure 2a. A large vortex is at this instant positioned close to the base of the airfoil, creating a large negative pressure and thereby a large drag. This is in contrast to Figure 2b, which is at a time when the C_d is at a local minimum. Applying flow control with an oscillatory jet resulted in reduced size and strength of the global vortices. Moreover, the global vortices would typically form further downstream, overall resulting in drastically reduced drag on the airfoil. A representative view of the instantaneous pressure contours with the oscillatory jet applied is shown in Figure 2c. The same trend is seen by looking at the instantaneous iso-pressure surfaces for the unforced case in Figure 3a, while with the forcing on in Figure 3b there are no iso-pressure surfaces in the vicinity of the base of the airfoil. The contour levels had identical settings for both the unforced and forced cases. Notice the strong small vortices on the flap created by the oscillatory slot jet. In this case, the slot jet oscillated in phase along the whole span, making the flow control vortices rather two-dimensional. Looking at time-averaged pressure contours in the middle of the domain, it is also seen in Figure 4a that a low-pressure region is present downstream of the airfoil for the unforced case, and much weaker with the AFC forcing on in Figure 4b.

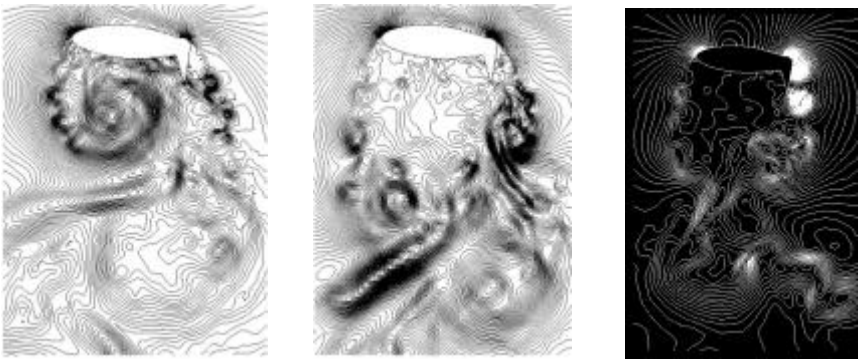

Figure 2 Instantaneous pressure contours. a) C_d at local maximum, no forcing b) C_d at local minimum, no forcing c) With forcing

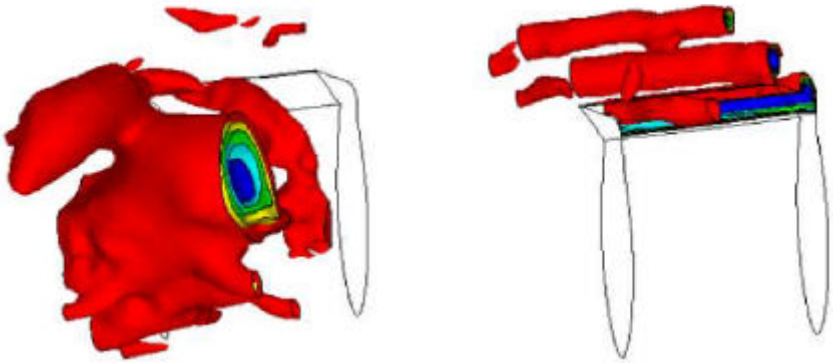

Figure 3 Iso-surfaces of instantaneous pressure. a) without AFC b) with AFC

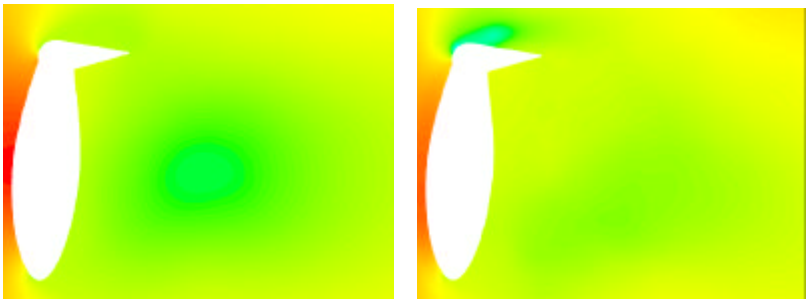

Figure 4 Time-averaged pressure contours. a) Without forcing b) With forcing

Based on this, it was not surprising that the instantaneous pressure at a point in the middle of the base of the airfoil correlated very well with the total CD of the whole airfoil, as was shown computationally (for instantaneous pressure) and also experimentally (for time-averaged pressure) in [9].

Time-history of the drag coefficient in Figure 5 shows that the C_d fluctuations were rather large and of a random nature, as can be expected from reality and from an LES calculation. With the oscillatory forcing jets on, these fluctuations were significantly reduced, another result of the reduced global vortex shedding.

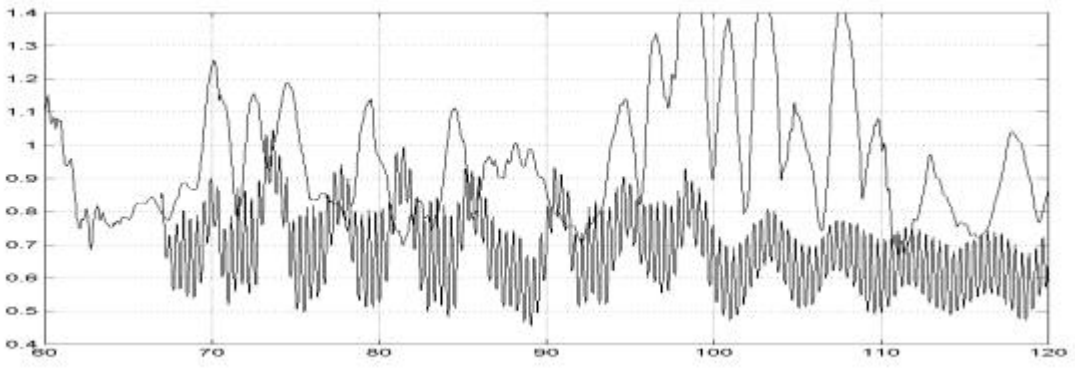

Figure 5 Time-histories of (normalized) drag coefficient. Rapid oscillations correspond to forced case. Forcing starts at tU/c=67.

Using a design-of-experiment/response surface method, the influence of slot angles and forcing frequencies F^+ were analyzed, Figure 6a. Here it is seen that the optimal forcing frequency was ~F^+~0.5. The LES code is interfaced with the optimization tools in ANSYS, and using more variables, i.e. slot angle, forcing frequency, and coordinates of up to 4 points on a spline modeling the surface from the slot to the trailing edge of the flap gave the design suggestions shown in Figure 6b and 6c, where the drag coefficients were reduced to 64% and 55% of its baseline value without flow control. Similar results were also obtained with the response surface method. It should be mentioned that in a strict mathematical sense, the ANSYS optimization tools used might not be able to find neither the global nor the local optimum. However, it is a very useful tool to find suitable designs.

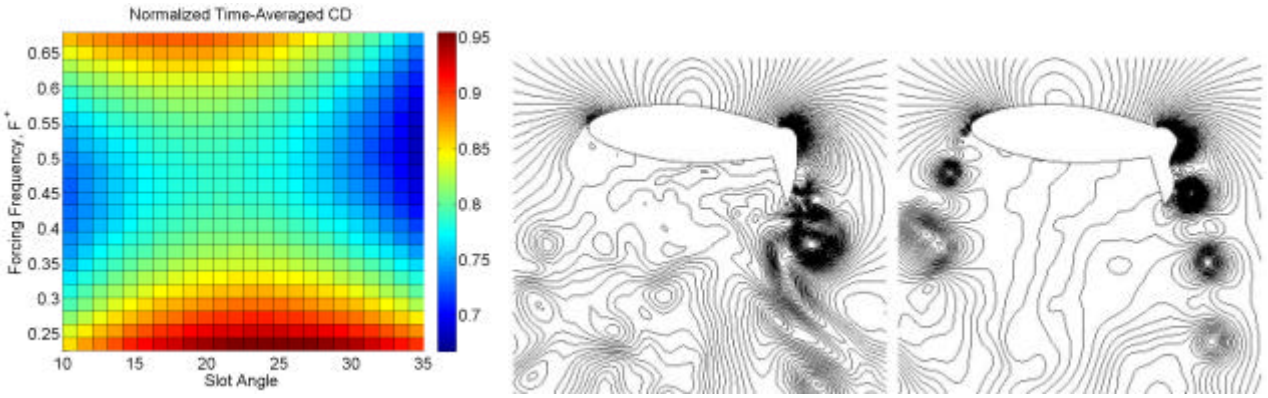

Figure 6 a) Response surface method: slot angle & forcing frequency vs. C_d. b) pressure contours for design suggested by ANSYS using 3 optimization variables c) pressure contours for design suggested by ANSYS using 6 optimization variables

Conclusions

The flow fields for a XV-15 airfoil with and without zero mass-flux oscillatory jets as flow control actuators were analyzed with numerous large eddy simulations. Without the oscillatory jets, typical bluff body aerodynamics characteristics are present, such as large drag, strong global vortex shedding, relatively large fluctuations in drag and lift. However, with the forcing jets, the global vortex shedding is greatly reduced, drag is reduced, and fluctuations in drag and lift are reduced. Using design & shape optimization tools, the optimal forcing frequency was found to be around F+~0.5, and the optimal slot angle either very small (<15 degrees) or around 35 degrees.

Acknowledgements

This work is supported by the Swedish Agency of Innovation Systems (VINNOVA), Volvo Trucks/3P, and SKAB. Financial support by SNIC for computer time at C3SE is gratefully acknowledged.

References

[1] T.L. Wood and M.A. Pereya. “Reduction of Tilt-rotor Download”. AHS 49th Annual Forum, 1993.
[2] M.A. McVeigh. “The V-22 tiltrotor large scale rotor performance wing/download test and comparison with theory”. 11th European Rotorcraft Forum Paper 97, London, 1985.
[3] M. Maisel, G. Laub, and W. J. McCroskey. “Aerodynamic characteristics of two-dimensional wings at angle of attack near 90 degrees”. NASA TM 88373, 1986.
[4] W. J. McCroskey, P. Spalart, G. Laub, and M. Maisel. “Airloads on bluff bodies with application to the rotor induced downloads on tilt-rotor aircraft”. Vertica, 9:1-11, 1985.
[5] R. Wall. “Tiltrotor Tech”, Aviation Week & Space Technology, May 26 2003, p. 30.
[6] E. H. Phillips. “DARPA Dumps Drag”, Aviation Week & Space Technology, July 21 2003, p. 30.
[7] P. Kjellgren, N. Anderberg, and I. Wygnanski. ”Download Alleviation by Periodic Excitation on a Typical Tilt-Rotor Configuration – Computation and Experiment”. AIAA paper 2000-2697, 2000.
[8] P. Kjellgren, D. Cerchie, L. Cullen, and I. Wygnanski. “Active Flow Control on Bluff Bodies With Distinct Separation Location”. AIAA paper 2002-3069, 2002.
[9] P. Kjellgren, A. Hassan, J. Sivasubramanian, L. Cullen, D. Cerchie, and I. Wygnanski. “Download Alleviation For The XV15: Computations and Experiments of Flows Around The Wing”, AIAA 2002-6007.
[10] M. El-Alti, P. Kjellgren, L. Davidson. “On the Download Alleviation for the XV-15 Wing by Active Flow Control Using Large Eddy Simulation”, ERCOFTAC Workshop on Direct and Large-Eddy Simulation, Trieste, Italy, September 8-10, 2008.
[11] P. Kjellgren. “A semi-implicit fractional step finite element method for viscous incompressible flows”. Computational Mechanics, 20:541-550, 1997.
[12] P. Kjellgren and J. Hyvarinen. “An Arbitrary Lagrangian-Eulerian Finite Element Method”. Computational Mechanics, 21:81-90, 1998.
[13] Lilly, D. K. “A Proposed Modification of the Germano Subgrid-Scale Closure Method”. Phys. Fluids A 4(3), 633-635, 1992.